MAGNETIC RESONANCE
Open Access
Discussions

Mechanical ordering of pigment crystallites in oil binder: Can EPR reveal the gesture of an artist?

Elise Garel, Laurent Binet and Didier Gourier

5   Chimie-ParisTech, PSL University, CNRS, Institut de Recherche de Chimie-Paris, F-75005 Paris, France

Correspondence to: Laurent Binet (laurent.binet@chimieparistech.psl.eu)

Abstract. Is it possible to reconstruct the gesture of an ancient artist applying a paint layer, considering that the orientation
10   distribution of crystallites of an inorganic pigment remains definitively imprinted on the support after drying of the layer? If
the pigment contains paramagnetic transition metal ions whose magnetic interactions are themselves anisotropic, then the
shape of the EPR spectrum should reflect the distribution of grain orientations. We have demonstrated this effect in the case
of Egyptian blue $CaCuSi_4O_{10}$, a pigment used for at least three millennia in antiquity, by reconstructing the probability density
of crystallite orientations under various modes of application**,** such as brush-painting, dabbing and droplet deposition.

15

1. Introduction

In magnetic resonance, including Electron Paramagnetic Resonance (EPR), the interactions contained in the spin Hamiltonian
are essentially anisotropic. For a system in a rigid state, much information on the structure at the molecular scale of the observed
species can be obtained from the anisotropic parts of these interactions. The anisotropic interactions can also be helpful to
20   analyze the orientation distributions of paramagnetic species in disordered materials, thus providing information on the
texturation of the sample at a macroscopic scale (Hentschel, et al., 1978; Friesner, et al., 1979). For instance, EPR has already
been used to investigate ordering in liquid crystals (Meirovitch, et al., 1982; Imrie, et al., 1997; Yankova, et al., 2013;
Bogdanov and Vorobiev, 2022), in polymer films (Vorobiev and Chumakova, 2005), in muscle fibers (Fajer, 1994), in oriented
bacteria (Franck et al., 1979) or of graphene oxide membranes (Chumakova, et al., 2022). This approach should also be fruitful
25   in the field of cultural heritage where complex composite magnetic materials are often to be found in cultural artifacts. As an
example, paintings are generally made of layers of pigment grains dispersed in a polymer binder. Most often pigments contain
paramagnetic transition ions as coloring species. It can be expected that the orientation of the inorganic grains within the layer
is not random but rather keeps the memory of the painter's gesture. Therefore, analyzing the orientation distribution of pigment
grains within a painting would potentially provide useful information on the making. In this paper, we aim at testing the
30   potential of EPR in determining the orientation distributions of pigment grains in a polymer film. The chosen system is

cuprorivaite $CaCuSi_4O_{10}$ also known as Egyptian blue, a pigment widely used in the Mediterranean basin since about 2500 BC (4th Egyptian dynasty) until the end of the Roman empire, its manufacturing recipe having been lost around the seventh century AD (Pagès-Camagna and Colinart, 2003). In this work we study by EPR the orientation effects of cuprorivaite crystallites dispersed in dried linseed oil binder. Different deposition modes of the mixture on a substrate were tested to investigate their

35 influence on the orientation distribution.

2. Experimental procedures

2.1. Sample preparation

The Egyptian blue pigment was synthetized by solid-state reaction from calcium carbonate $CaCO_3$, amorphous silica SiO_2,

40 copper oxide CuO and 3 w.\% of sodium carbonate Na_2CO_3. The powders were mixed and ground together then pressed into pellets under a uniaxial pressure of 4 tons/cm^2. The pellets were first sintered in air at 1000 °C for 5h. The resulting samples were then ground, pressed into new pellets, and sintered again during 17 h in air at 1000 °C. After this final sintering, the samples were ground again in powder. The purity of the material was tested by X-ray diffraction (XRD) using an X Panalytical X'Pert Pro diffractometer with the $K_{\alpha 1}$ ray of a copper anticathode ($\lambda = 0.15406$ nm). XRD patterns show that the synthesized

45 powder consists of cuprorivaite $CaCuSi_4O_{10}$ with traces of wollastonite $CaSiO_3$ and SiO_2 (Binet et al., 2021). The as-obtained Egyptian Blue pigment was then mixed with boiled linseed oil as a binder in proportion of 10 w.\% of pigment.

The mixture was deposited on either a glass plate or on a semi-rigid transparent polymer substrate (transparency for overhead projector) in four different ways (Fig. 1): (i) a one-way spreading with a film applicator to produce a 250 µm thick (before drying) film, (ii) a one-way spreading with a paintbrush, (iii) a dabbing with a paintbrush, (iv) a droplet deposition with a

50 pipette. The samples were then let dry for several days until the linseed oil becomes rigid. For EPR analysis, small pieces with dimensions 25 mm x 2-3 mm were cut perpendicularly to the spreading direction (when relevant) as shown in Fig. 1.
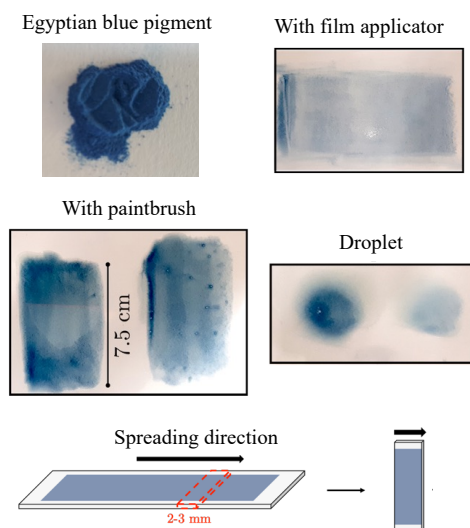

Figure 1. Photographs of the samples

MAGNETIC RESONANCE
Open Access Discussions

2.2. EPR analysis

55 EPR spectra were recorded at room temperature with a Bruker Elexsys E500 spectrometer equipped with Bruker SHQE resonator operating at X-band (microwave frequency ≈ 9.25-9.39 GHz depending on the sample). The applied magnetic field was modulated at 100 kHz with a 1 mT amplitude for lock-in detection. The microwave power was 2 mW. To analyze theoretically the orientation distribution of pigment grains in a fluid medium, a sample made of pigment powder in fluid linseed oiled was submitted to a 20 mT magnetic field in the EPR spectrometer, at room temperature. Then the sample was cooled

60 down to 200 K with gaseous nitrogen to freeze the oil and to keep the grain orientations fixed in the sample. EPR spectra at different orientations of the sample in the external field were then recorded at this temperature.

All calculations for EPR spectra analysis were performed with Matlab (script given in Supplementary Information). The Easyspin package (Stoll and Schweiger, 2006) was used for EPR spectrum simulation, by taking an axial g-matrix with principal values $g_x = g_y = 2.055 = g_\perp$ and $g_z = 2.350 = g_\parallel$ for Cu^{2+} in the Egyptian Blue pigment. Here the (x, y, z)

65 molecular frame is such as the z-axis is the C_4 symmetry axis of the Cu^{2+} coordination site with D_{4h} symmetry (Ford and Hitchman, 1979). This axis is also the crystal c-axis of the structure (Pabst, 1959). A Voigt line shape was considered for the EPR transitions with an empirical dependence of the peak-to-peak width ΔB on the angle θ between the applied field and the z-axis as $\Delta B = 0.86 + \sqrt{0.37\cos^2\theta + 0.12\sin^2\theta}$ (in mT), for both Lorentzian and Gaussian components.

70 **3. Theoretical background for orientation distribution analysis**

3.1. EPR spectrum of a powder sample with random orientation distribution of the crystallites

The EPR of the Cu^{2+} ion in cuprorivaite can be described by a spin Hamiltonian including only the Zeeman interaction with the external applied magnetic field $\vec{B}$:

$$\widehat{H} = \mu_B \vec{B} \cdot \boldsymbol{g}\vec{S} \tag{1}$$

75 where μ_B is the electron Bohr magneton, $\boldsymbol{g}$ the electron g-factor matrix and $\vec{S}$ the electron spin. The hyperfine interaction with the central nucleus ^{63}Cu or ^{65}Cu is not to be considered in the Hamiltonian as it is averaged out by exchanged interaction between Cu^{2+} ions (Binet, et al., 2021). The resonance field is then determined by the g-factor only and its anisotropy. An EPR spectrum is recorded by scanning the applied field at fixed frequency ν of the electromagnetic wave. For the magnetic field making an angle θ with the molecular z-axis, an EPR transition occurs at a resonance magnetic field

80
$$B_r(\theta) = \frac{h\nu}{\mu_B\sqrt{g_\parallel^2\cos^2(\theta) + g_\perp^2\sin^2(\theta)}} \tag{2}$$

with h the Planck constant. The resonance field thus varies in a range defined by the boundary values $B_r^\parallel = B_r(\theta = 0) = h\nu/g_\parallel\mu_B$ and $B_r^\perp = B_r\left(\theta = \frac{\pi}{2}\right) = h\nu/g_\perp\mu_B$ with $B_r^\parallel < B_r^\perp$ in the present case. The EPR transition of a Cu^{2+} ion thus depends on the orientation of the molecular frame (x, y, z) within the laboratory frame (X_0, Y_0, Z_0) defined such as $\vec{B} \parallel Z_0$, through the

angle θ. In the case of a powder sample where crystallites exhibit a perfectly random distribution of orientations, the EPR
85   spectrum is given by summing over all possible orientations θ:

$$S(B) = \int_{\theta=0}^{\pi/2} \omega(\theta) f\big(B - B_r(\theta)\big) \sin\theta \, d\theta \tag{3}$$

where $f\big(B - B_r(\theta)\big)$ is a normalized lineshape function, and $\omega(\theta)$ is the transition probability. A typical EPR spectrum in the
case of a random distribution of crystallite orientations and for an axial g-matrix is shown in Fig. 2. It exhibits a low-field
maximum at $B_r^{\parallel}$ and a baseline crossing close to (but not exactly at) $B_r^{\perp}$.
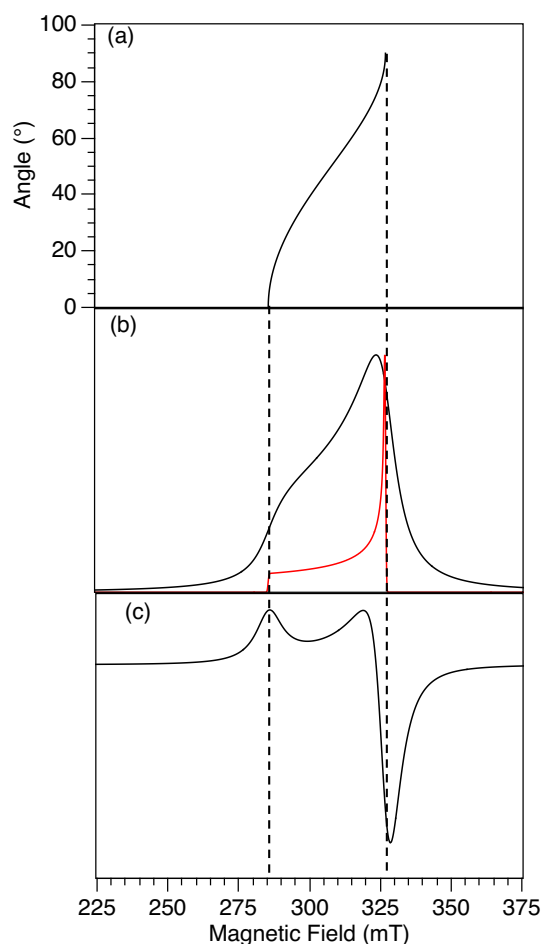

90

Figure 2: (a) Angular variation of the EPR resonance field according to Eq. 2. for Cu^{2+} in cuprorivaite. (b) Spectral density in
red and corresponding EPR absorption spectrum in black considering a non-zero linewidth. (c) Actual EPR spectrum
corresponding to the absorption derivative.

3.2. Powder EPR spectrum with preferred orientation of the crystallites

To describe the EPR spectrum of a sample with a non-random distribution of crystallites orientations, three different frames need to be considered, namely the molecular frame (x, y, z), the sample frame (X, Y, Z) with X, Y and Z axes having a defined position with respect to the sample, and the laboratory frame (X_0, Y_0, Z_0), as shown in Fig. 3a. The orientation of the molecular frame within the sample frame is specified by a set of three Euler angles $\Omega = (\alpha, \beta, \gamma)$, its orientation within the laboratory frame by the set $\Omega' = (\varphi, \theta, \psi)$ and the orientation of the sample frame within the laboratory frame by the set $\Omega_0 = (\alpha_0, \beta_0, \gamma_0)$ (Fig. 3b).
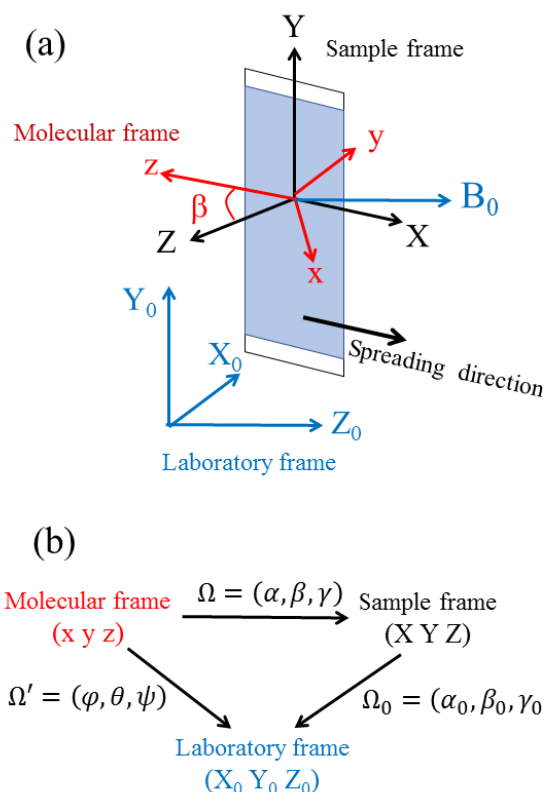

Figure 3. (a) Definition of the molecular, sample and laboratory frames. (b) Sets of Euler angles relating the various frames.

The relevant quantity to characterize the non-random orientations is the orientation probability density $\mathcal{P}(\Omega)$ of the crystallites in the sample frame (X, Y, Z) such that $\mathcal{P}(\Omega)d\alpha \sin\beta \, d\beta d\gamma$ is the probability of the molecular frame orientation in the sample frame being found in the range $[\alpha, \alpha + d\alpha[\times [\beta, \beta + d\beta[\times [\gamma, \gamma + d\gamma[$. This density $\mathcal{P}(\Omega)$ is directly related to the way the pigment was applied on the sample. It is normalized so that $\int_{\alpha=0}^{2\pi} \int_{\beta=0}^{\pi} \int_{\gamma=0}^{2\pi} \mathcal{P}(\Omega)d\alpha \sin\beta \, d\beta d\gamma = 1$. For a specific orientation $\Omega_0 = (\alpha_0, \beta_0, \gamma_0)$ of the sample in the laboratory frame, the EPR spectrum is then given by:

$$S(B, \Omega_0) = \int_\Omega \mathcal{P}(\Omega)\omega(\Omega, \Omega_0)f\big(B - B_r(\Omega, \Omega_0)\big)d\Omega \tag{4}$$

In the case of a random orientation distribution, $\mathcal{P}(\Omega)$ is constant with $\mathcal{P}(\Omega) = 1/8\pi^2$ and can be omitted in Eq. 4, which then reduces to Eq. 3. The determination of $\mathcal{P}(\Omega)$ from experimental EPR spectra is essentially adapted from Hentschel, et al. (1978). The unknown probability density $\mathcal{P}(\Omega)$ is first expanded as a combination of Wigner matrice elements $D_{mn}^{(l)}(\Omega)$:

$$\mathcal{P}(\Omega) = \sum_{l=0}^\infty \sum_{m=-l}^l \sum_{n=-l}^l p_{lmn}D_{mn}^{(l)}(\Omega) \tag{5}$$

where $D_{mn}^{(l)}(\alpha, \beta, \gamma) = e^{-im\alpha}e^{-in\gamma}\langle Y_{l,m}|\exp(-i\beta\hat{L}_y/\hbar)|Y_{l,n}\rangle$, $Y_{l,m}$ and $Y_{l,n}$ being spherical harmonics and $\hat{L}_y$ the y-component of the orbital angular momentum operator. An essential simplification can be introduced here because all samples happened to have a revolution symmetry about the Z-axis of the sample frame (see below). The probability density $\mathcal{P}(\Omega)$ then no longer depends on α and γ but only on β. This implies $m = n = 0$ and:

$$\mathcal{P}(\Omega) = \mathcal{P}(\beta) = \sum_{l=0}^\infty p_l D_{00}^{(l)}(\Omega) \tag{6}$$

where $D_{00}^{(l)}(\Omega) = P_l(\cos\beta)$ with $P_l(x)$ being the l-th order Legendre polynomial. The orientation probability density $\mathcal{P}(\Omega)$ is then fully determined by the set of coefficients p_l with $l \in \mathbb{N}$, which must be obtained from experimental EPR spectra. Detailed calculations given in Supporting Information show that the EPR spectrum for a specific orientation $\Omega_0 = (\alpha_0, \beta_0, \gamma_0)$ of the sample in the laboratory frame is given by:

$$S(B, \Omega_0) = S(B, \beta_0) = \sum_{l=0}^\infty p_l P_l(\cos\beta_0) \int_{\theta=0}^\pi \omega(\theta)f\big(B - B_r(\theta)\big)P_l(\cos\theta)\sin\theta \, d\theta \tag{7}$$

From the above equation, the EPR spectrum only depends on the angle β_0 between the sample Z-axis and the applied magnetic field. Therefore, only a set of spectra at different β_0 angles are needed to determine the p_l coefficients. The numerical implementation of the determination of the p_l coefficients from a set of experimental spectra at different orientations β_0 of the sample in the laboratory frame is given in Supporting Information. It should be however noticed that since the EPR phenomenon is unchanged by reverting the orientation of the applied field, only p_l coefficients with l even can be determined so that the actual probability density $\mathcal{P}(\Omega)$ cannot be fully obtained from EPR.

4. Orientation distribution of pigment crystallites in fluid oil under magnetic field

The determination of the preferred orientation of pigment crystallites is illustrated in the case of cuprorivaite crystallites dispersed in a fluid medium, such as oil, and oriented by an external magnetic field. Under an external field, the magnetic potential energy per unit volume of a crystallite is

$$E(\theta) = -Ng(\theta)\mu_B B\langle S_z \rangle = -\frac{1}{2}Ng(\theta)\mu_B B \tanh\left(\frac{g(\theta)\mu_B B}{2kT}\right) \tag{8}$$

6

**MAGNETIC
RESONANCE**
Open Access
Discussions

where N is the number of Cu^{2+} ions per unit volume, $\langle S_z \rangle$ the thermal average of the Cu^{2+} electron spin component along the magnetic field direction. In a fluid, a pigment crystallite is free to rotate to minimize its potential energy. It appears from Eq. 8 that the potential energy is minimal for an orientation θ of the molecular z axis with respect to the field corresponding to the

140   maximum value of the g-factor $g(\theta = 0) = g_\parallel$. Therefore, we expect pigment crystallites to be mostly oriented so that their crystal c-axis (which is parallel to the molecular z-axis) is along the applied field, which here defines the sample Z-axis. After orientation in the field, the sample was cooled to freeze the oil and thus the grain orientations, and EPR spectra were recorded upon varying the angle β_0 between the measuring field (Z_0 direction) and the sample Z axis. These spectra are shown in Fig. 4 for different values of β_0.
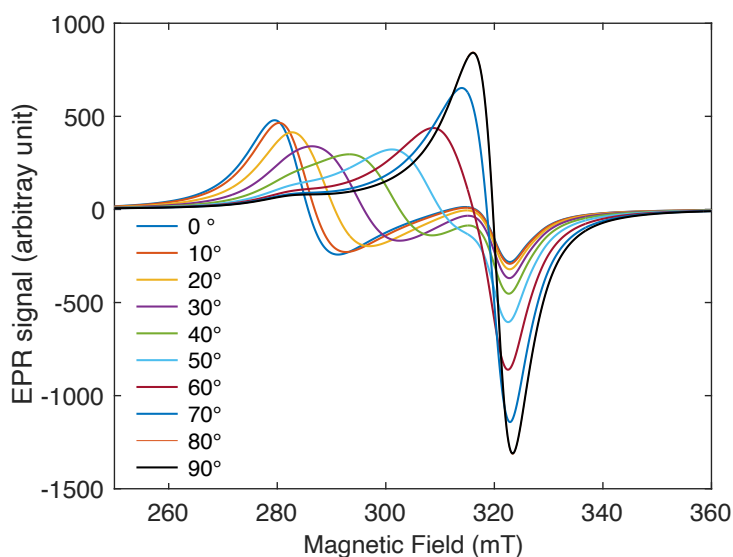

145

Figure 4. EPR spectra of frozen cuprorivaite grains magnetically oriented in oil for different angles β_0 between the orienting and the measuring fields.

For $\beta_0 = 0$ (measuring field parallel to the orienting field), the spectral density is mostly concentrated about the lowest

150   resonance field $B_r^\parallel = \frac{h\nu}{g_\parallel \mu_B}$. When the angle β_0 increases up to $\frac{\pi}{2}$, the EPR spectral density shifts to higher fields, and is concentrated about the highest resonance field $B_r^\perp = h\nu/g_\perp \mu_B$ at $\beta_0 = \frac{\pi}{2}$ (measuring field perpendicular to the orienting field). This angular dependence of the EPR spectra shows that, as expected, crystallites have been predominantly oriented with their crystal c-axis along the orienting field. The orientation probability density $\mathcal{P}(\beta)$ calculated from the EPR spectra is shown in Fig. 5a, where β is also here the angle between the crystal c-axis and the orienting field. The calculated EPR spectra are given

155   in Fig. S1. The polar representation of $\mathcal{P}(\beta)$ shows a large maximum of $\mathcal{P}(\beta)$ for $\beta = 0$ and can be compared to the probability density for a random distribution of orientations (red circle in the middle of Fig. 5a). This clearly indicates a strongly anisotropic orientation distribution of the pigment grains. Figure 5b shows the p_l coefficients in the expansion of $\mathcal{P}(\beta)$ in Eq.

6. Order $l = 0$ corresponds to the isotropic contribution to $\mathcal{P}(\beta)$ and values $l \neq 0$ to the anisotropic components. The highly anisotropic character of $\mathcal{P}(\beta)$ is shown by the fact that the isotropic component $l = 0$ is not the dominant one but rather components with l from 2 to 10.
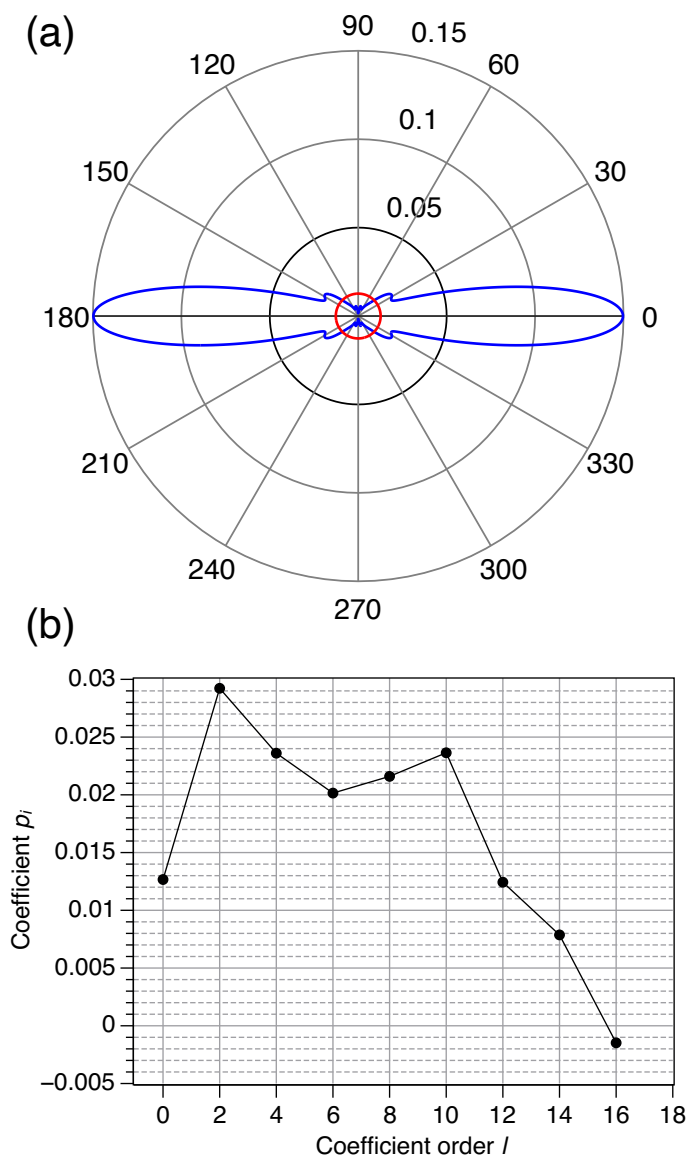

Figure 5. (a) Polar plot (in blue) of the orientation probability density $\mathcal{P}(\beta)$ for cuprorivaite magnetically oriented in fluid oil. The red circle represents a perfectly random orientation distribution $\mathcal{P}(\beta) = 1/8\pi^2$. (b) Coefficients p_l in the expansion of $\mathcal{P}(\beta)$ according to Eq. 6.

5. Orientation distribution of pigment grains in dried films: effect of the application process

5.1. Films deposited with the applicator

Films were deposited on a flat substrate with an applicator by a one-way spreading along the *X*-direction in the substrate plane (Fig. 3a) of a mixture of fluid linseed oil and pigment grains. This application process is expected to be the most reproducible

170   one among those used in this work. Since an anisotropy along the *X*-direction is induced by the process, it is meaningful to determine if a preferred orientation of the grains is induced and how the distribution is oriented with respect to the spreading *X*-direction. EPR spectra corresponding to the rotation of the sample about the sample *Z*-axis and about the sample *Y*-axis are shown in Figs. 6a and 6b, respectively. It turns out that there is no significant change in the spectrum shape upon rotation about the *Z*-axis (Fig. 6a). This means that the orientation distribution has a revolution symmetry about the *Z*-axis.
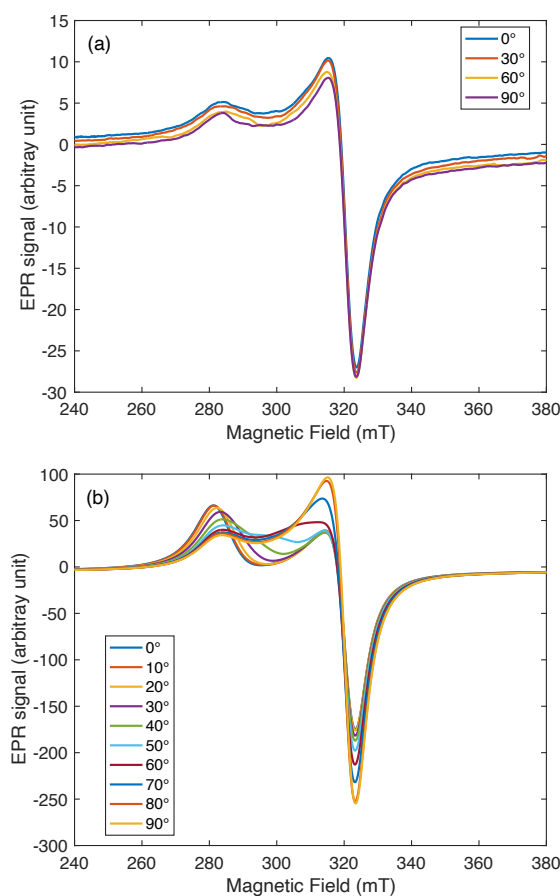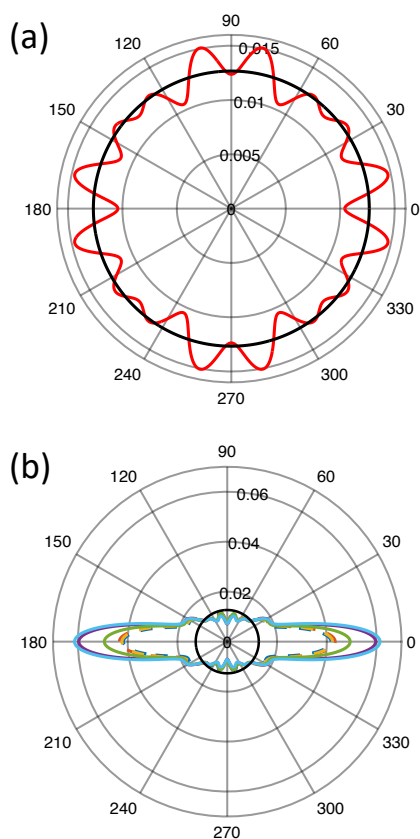

175

Figure 6. EPR spectra of a film deposited with an applicator upon rotation about (a) the *Z*-axis, (b) the *Y*-axis, at different angles β_0 between the magnetic field and (a) the *X*-axis or (b) the *Z*-axis.

Figure 7. Orientation probability densities $\mathcal{P}(\beta)$ for 6 films deposited under same conditions with an applicator calculated from (a) a rotation of the sample about the Z-axis (β being the angle from the X-axis in the XY-plane), (b) a rotation about the Y-axis (β being the angle from the Z-axis in the XZ-plane). The black circles correspond to a random orientation.

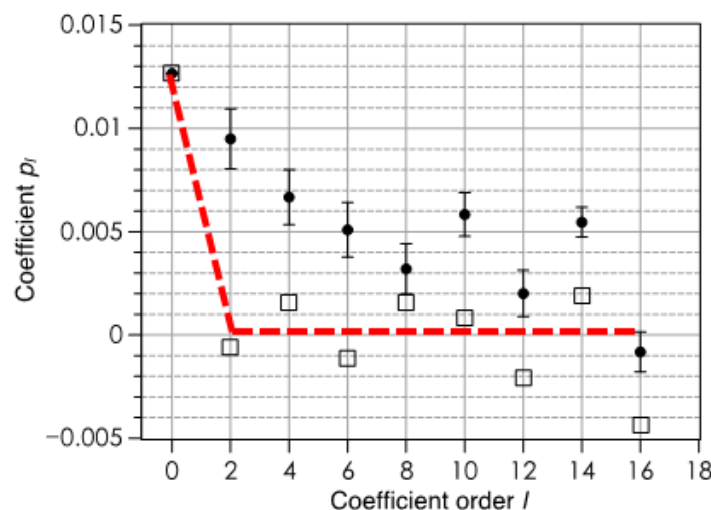**MAGNETIC
RESONANCE**
Discussions

Figure 8. Coefficients p_l in the expansion of $\mathcal{P}(\beta)$ according to Eq. 6 for a rotation about the *Z*-axis (open squares) and a rotation about the *Y*-axis (black circles) in the case of films deposited with an applicator. The discontinuous red line corresponds to a random distribution of orientations.

This is confirmed by the polar plot of the corresponding density $\mathcal{P}(\beta)$ (here β is the angle from the *X*-axis in the *XY*-plane), which very close to a circle (Fig. 7a) and by the p_l coefficients close to zero except for $l = 0$ (Fig. 8). In this figure, the values of p_l coefficients corresponding to a random distribution of crystallite orientations are represented by a discontinuous red line. Significant changes in the EPR spectrum shape are observed upon rotation about the *Y*-axis, the magnetic field direction moving from the *Z*-direction ($\beta_0 = 0$) perpendicular to the sample plane to the *X*-direction ($\beta_0 = \pi/2$) in the sample plane (Fig. 6b). The low field part of the spectrum, corresponding to crystallites with the *c*-axis parallel to the field is enhanced at $\beta_0 \approx 0$, while the high field part (crystallites with the *c*-axis perpendicular to the field) is enhanced at $\beta_0 \approx \pi/2$. This means that crystallites are mostly oriented with their *c*-axis perpendicular to the sample plane. This is confirmed by the probability density $\mathcal{P}(\beta)$ being maximum at $\beta = 0$ (Fig. 7b). An example of calculated EPR spectra is given in Fig. S2 in the Supporting Information. The variability in the preferred orientation of the crystallites has been analyzed in a set of six samples prepared under the same conditions and the corresponding $\mathcal{P}(\beta)$ densities shown in Figure 7b with different colors. The average values of the p_l coefficients over those six samples are plotted in Figure 8 with the error bars given by their standard deviation. The maximum value $\mathcal{P}(\beta = 0) = 0.04 - 0.06$ of the probability density for the films is lower than in the case of magnetically oriented grains in fluid oil where the maximum value was $\mathcal{P}(\beta = 0) \approx 0.15$. For films, the highest value of p_l is at $l = 0$ corresponding to the isotropic contribution to $\mathcal{P}(\beta)$, while for magnetically oriented grains in fluid oil the anisotropic contributions at non-zero orders $l = 2 - 10$ dominate the isotropic one (Fig. 5b). All these results indicate that the preferred

grain orientation in dried films after mechanical application is less pronounced than under an external magnetic field in fluid
205 oil.

5.2. Preferred orientations with manual deposition modes

The preferred orientation with more operator-dependent modes of deposition were also investigated, namely spreading along
the X-direction in the sample plane with a paintbrush, dabbing onto the substrate with a paintbrush and droplet deposition with
210 a pipette. In each case two or three samples were prepared and analyzed. All samples exhibited a revolution symmetry about
the Z-axis as in the case of films deposited with the applicator. The EPR spectra under rotation about the Y-axis are given in
Figs S3 to S5 in the Supplementary Information. The orientation probability densities are shown in Figures 9a and 9b and the
corresponding p_l coefficients (average values over 2-3 samples and standard deviations as error bars) in Fig. 10.
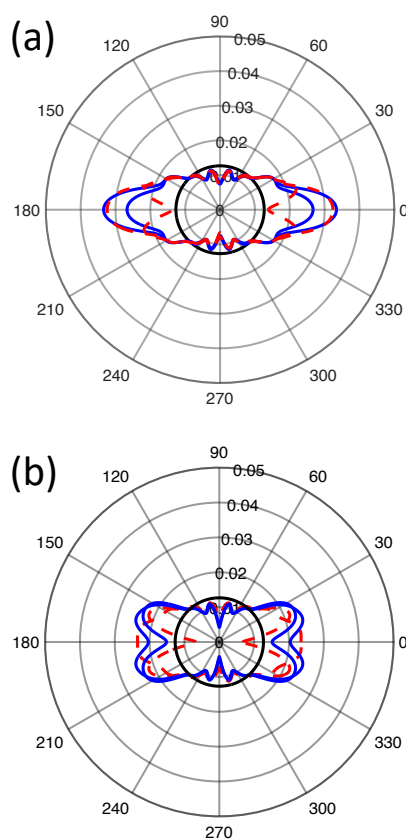

215 **Figure 9.** Orientation probability densities $\mathcal{P}(\beta)$ for films made by (a) brush-painting (full blue curves) and strong brush-painting (dashed red curves), (b) dabbing (full blue curves) and droplet deposition (dashed red curves). The black circles correspond to a random orientation distribution.

MAGNETIC
RESONANCE
Discussions

In all cases, the probability densities $\mathcal{P}(\beta)$ exhibit a maximum value for β in the range $0 - 17°$. This again shows a preferred

220   orientation with the crystal c-axis close to the sample Z-axis. However, the maximum values of $\mathcal{P}(\beta)$, about $0.02 - 0.03$ are

significantly lower than for films deposited with the applicator. This is in line with the p_l coefficients for $l \neq 0$ in Fig. 10,

which are lower than for films deposited with the applicator showing that the orientation distribution with paint-brushing,

dabbing or droplet deposition is less anisotropic than when the film is deposited with an applicator. When using a paintbrush,

increasing the strength of the gesture ("Strong brush-painting" data as compared to "Brush painting" data in Figs. 9a and 10)

225   does not seem to induce a significant difference in the orientation distribution, as shown by close $\mathcal{P}(\beta)$ curves in Fig. 9a and

almost equal leading p_l coefficients for $l = 2,4,6$ in Fig. 10. The orientation distributions in the cases of dabbing and droplet

deposition appear to be slightly less anisotropic than for brush-painting for their maximal values of $\mathcal{P}(\beta)$ are closer to the

lower bound 0.02 and for they have lower values of the leading p_l coefficients for $l = 2,4,6$.
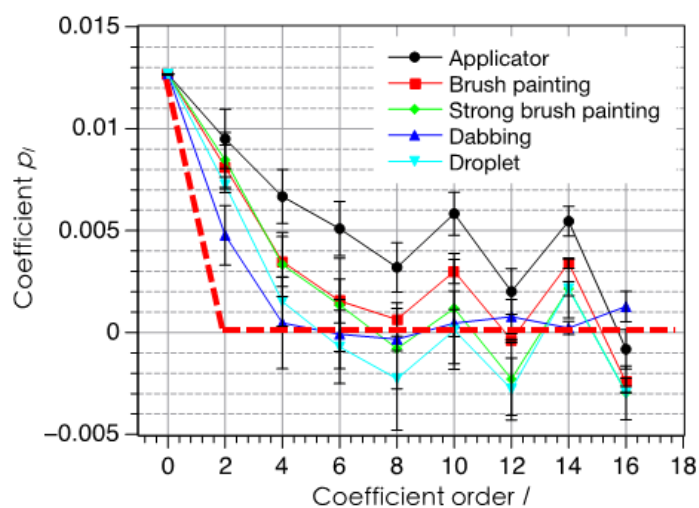

Figure 10. Coefficients p_l in the expansion of $\mathcal{P}(\beta)$ according to Eq. 6 for the various deposition modes of films. The

230   discontinuous red line corresponds to a random distribution of orientations.

5.3. Possible cause of the preferred orientation

Whatever the application mode of the oil-pigment mixture, two common features were revealed by the above analyzes: (*i*) the

235   pigment crystallites exhibit a preferred orientation with their crystal c-axes oriented almost perpendicularly to the sample

plane, (*ii*) the orientation distribution has a revolution symmetry about the normal to the sample plane. More surprising is that

these features are observed even when a mechanical stress is applied along the sample plane (X-axis) during the deposition

(whether with the applicator or with a paintbrush) and that this mechanical stress seems to induce the most pronounced

preferred orientations. It must also be mentioned that during the film deposition and drying, the Z-axis is along the vertical

240   direction so that the gravitational force is perpendicular to the sample plane. A possible explanation for this preferred

orientation is based on the sedimentation of the pigment crystallites within the oil while the latter is still viscous. Indeed,

microcrystals of cuprorivaite exhibit a tabular morphology (Bloise, et al., 2016). Then when microcrystals fall through the liquid oil under the gravitational force, they tend to lay down with their largest face horizontal (Fig. 11a). Consequently, microcrystals adopt a preferred orientation with the normal to the largest face perpendicular to the sample plane. The piling of

245   the crystals is not perfect, some crystals being tilted or aggregated in larger grains. This is mostly the case of the droplet or dabbing deposition. When a horizontal mechanical stress is applied with an applicator or a paint brush, the polymer chains of the oil get aligned along the stress direction (Fig. 11b). This may have two effects. First a dissociation of the aggregates into separate microcrystals, second a better alignment of the crystal tablets in the horizontal plane by polymer-crystal surface interactions. This could explain why the preferred orientation seems to be enhanced when such a mechanical stress is applied
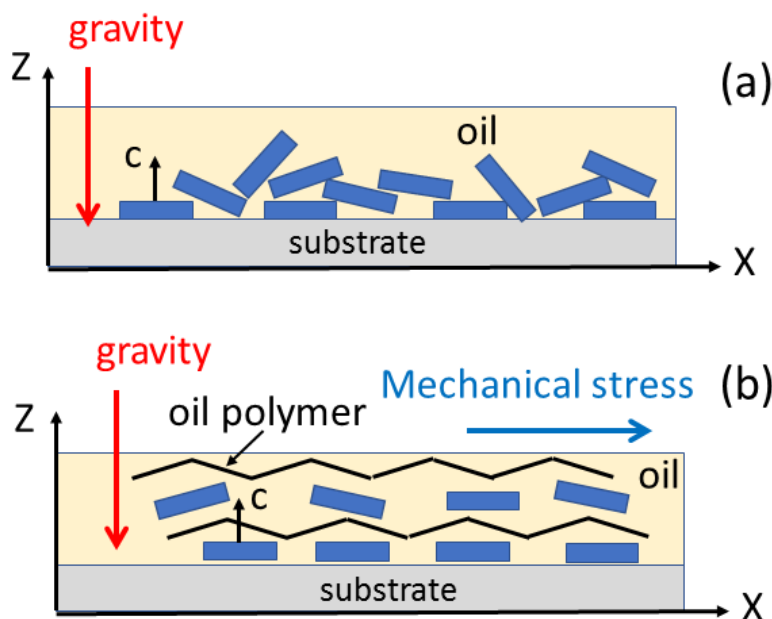
250   during film deposition.

Figure 11. Models for the sedimentation of pigment microcrystals in oil leading to (a) poorly oriented crystals upon dabbing or droplet deposition, (b) an enhanced orientation when the oil polymers are stretched by an in-plane mechanical stress in the case of brush-painting or deposition with an applicator.

255

5. Can EPR reveals the gesture of an artist?

We have seen that three competing forces can contribute to the preferential orientation of pigment grains in an organic binder: a magnetic field, gravity, and a mechanical stress. The orientation in a magnetic field could be potentially interesting if it is effective in the Earth field. However, in the present work on Egyptian blue pigment, we could hardly observe the orientation

260   effect in a field weaker than 20 mT, which is 1000 times higher than the earth field. The effect of gravity and mechanical strain

can induce a preferential orientation only if pigment grains have a symmetry lower than cubic, *i.e.* in the case of platelets, cylinders, rods etc... In the case of Egyptian blue, whose crystallites are in the form of platelets, these two forces orientate the platelets parallel to each other. Therefore, if the substrate is horizontal, gravity and mechanical stress will both orient the platelets parallel to the substrate, as shown in the experiments described in this work (Fig.11). Nonetheless, these two situations

265   can be distinguished by a careful analysis of the EPR lineshape, as shown above. However, the platelet-shape of the crystallites does not allow to identify the direction of the painter's gesture because the *z* axis of the platelets is perpendicular to the spreading gesture, whatever the direction of this movement. In principle, the relative effects of gravity and mechanical stress should be better differentiated if the support is vertical, which is generally the case for paintings and frescoes. In this situation, gravity should tend to orient the plates perpendicular to the substrate while the artist's gesture will orient them parallel to the

270   substrate.

The ideal case for determining artist's gesture by EPR would certainly be the case where pigment crystallites have the shape of elongated parallelepipeds, rods, cylinders, with an additional condition that the *z*-axis of the molecular frame is along the main axis of the crystallite. In the case of a horizontal substrate, it is anticipated that gravity will randomly orient the *z*-axes of the rods in the XY plane of the sample frame, while application of the pigment will orient the rods in the direction of the

275   gesture. One would then expect to obtain orientation probability densities that would precisely reflect the artist's intentions.

6. Conclusion

This work shows that the simple act of spreading a paramagnetic pigment dispersed in a binder on a surface introduces a preferential distribution of grains orientations on the paint layer that can be detected by EPR. This effect has been demonstrated

280   with Egyptian blue, a pigment that was used for several millennia in antiquity. By analyzing the variation of the EPR line shape as a function of the angle between the magnetic field and the surface of the layer, the orientation probability density of the grains can be determined and was found to deviate significantly from the random distribution. It is possible to differentiate between orientation distributions induced by mechanical spreading and those in which only gravity is at work (droplet deposition, dabbing). This effect has been demonstrated with a pigment (Egyptian blue) whose grains are in the form of

285   platelets. It would certainly be greater for rod-shaped grains.

Author Contributions.

Elise Garel prepared the samples and performed the EPR experiments. Elise Garel and Laurent Binet processed the data and performed the calculations. The three authors discussed and interpreted the results. Laurent Binet and Didier Gourier wrote

290   the paper. All authors have read and agreed to this version of the manuscript.

Competing interests. The authors declare no competing financial interest.

MAGNETIC RESONANCE
Open Access Discussions

Acknowledgment.

295

Supplementary information. Derivation of Eq.7; Numerical calculation of the coefficients p_l from experimental EPR
300   spectra; Matlab script for the calculation of the orientation probability density; Experimental and calculated EPR spectra;

References.

Binet L., Lizion J., Bertaina S., and Gourier D.: Magnetic and New Optical Properties in the UV–visible Range of the Egyptian

305   Blue Pigment Cuprorivaite CaCuSi$_4$O$_{10}$, J. Phys. Chem. C 15, 25189-25196, https://doi.org/10.1021/acs.jpcc.1c06060, 2021.

Bloise A., Abd El Salam S., De Luca R., Crisci G.M., and Miriello D.: Flux growth and characterization of cuprorivaite: the influence of temperature, flux, and silica source, Appl. Phys. A 122, 650, https://doi.org/10.1007/s00339-016-0198-1, 2016.

Bogdanov A. V. and Vorobiev A. Kh.: Orientation distribution of molecules in a smectic liquid crystal with a distorted director geometry, J. Phys. Chem. B 126, 2573, https://doi.org/ 10.1021/acs.jpcb.1c09795, 2022.

310   Chumakova N. A., Vorobiev A. Kh., Astvatsaturov D. A., Yankova T. S., Rebrikova A. T. and Matveev M. V.: Quantitative determination of the orientational ordering of graphene oxide membranes by the spin probe technique, Phys. Chem. Chem. Phys. 24, 4881, https://doi.org/10.1039/d1cp05417a, 2022.

Fajer, P.: Determination of spin-label orientation within the myosin head, Proc. Nat. Acad. Sci. 91, 937-941, https://doi.org/10.1073/pnas.91.3.937, 1994.

315   Ford, R., and Hitchman M.: Single crystal electronic and EPR spectra of CaCuSi$_4$O$_{10}$, a synthetic silicate containing copper(II) in a four-coordinate, planar ligand environment, Inorganica Chimica Acta 33, L167-L170, https://doi.org/10.1016/S0020-1693(00)89436-0, 1979.

Frank, H.A., Friesner, R., Nairn, J.A., Dismukes, G.C., and Sauer, K.: Biochimica et Biophysica Acta 547, 484-501, https://doi.org/10.1016/0005-2728(79)90029-X, 1979.

320   Friesner R., Nairn J.A., and Sauer K.: Direct calculation of the orientational distribution function of partially ordered ensembles from the EPR line shape, J. Chem. Phys. 71, 358-365, https://doi.org/10.1063/1.438078, 1979.

Hentschel R., Schlitter J., and Speiss H.W.: Orientational distributions in partially ordered solids as determined from NMR and ESR line-shapes, J. Chem. Phys. 68, 56-66, https://doi.org/10.1063/1.435473, 1978.

Imrie, C.T., Ionescu, D., and Luckhurst, G.R.: Molecular organization of the polymer backbone in a side group liquid crystal

325   polymer. An ESR investigation, Macromolecules 30, 4597-4600, https://doi.org/10.1021/ma970365c, 1997.

Meirovitch, E., Igner, D., Igner, E., Moro, G., and Freed, J.H.: Electron-spin relaxation and ordering in smectic and supercooled nematic liquid crystals, J. Chem. Phys. 77, 3915-3938, https://doi.org/10.1063/1.444346, 1982.

Pabst A.: Structures of some tetragonal sheet silicates, Acta. Cryst. 12, 733-739, https://doi.org/ 10.1107/S0365110X5900216X, 1959.

330 Pagès-Camagna, S., and Colinart, S.: The Egyptian green pigment: its manufacturing process and links to Egyptian blue, Archaeometry 45, 637-658, https://doi.org/10.1046/j.1475-4754.2003.00134.x, 2003.

Stoll, S., and Schweiger A.: Easyspin, a comprehensive software package for spectral simulation and analysis in EPR, J. Magn. reson. 178, 42-55, https://doi.org/ 10.1016/j.jmr.2005.08.013, 2006.

Vorobiev, A.K., and Chumakova, N.A.: Determination of orientation distribution function of anisotropic paramagnetic species

335 by analysis of ESR spectra angular dependence, J. Magn. Reson. 175, 146-157, https://doi.org/10.1016/j.jmr.2005.04.001, 2005.

Yankova, T.S, Chumakova, N.A., Pomogailo, D.A., and Vorobiev, A.K.: Orientational order of guest molecules in aligned liquid crystal as measured by EPR and UV-vis techniques, Liquid Crystals 40, 1135-1145, https://doi.org/10.1080/02678292.2013.795621, 2013.

340